JOURNAL OF APPLIED ELECTROCHEMISTRY **21** (1991) 335–345

Characterization of DSA®-type oxygen evolving electrodes: choice of a coating

CH. COMNINELLIS*, G. P. VERCESI

Institute of Chemical Engineering, Swiss Federal Institute of Technology, CH-1015 Lausanne, Switzerland

Received 12 June 1990; revised 2 September 1990

In the search for a DSA®-type electrode for oxygen evolution in acidic solutions, nine binary coatings with IrO_2, RuO_2, Pt as conducting component, and TiO_2, ZrO_2, Ta_2O_5 as inert oxides, have been deposited on titanium, examined for their microstructural properties and tested for their electrocatalytic activity and anodic stability. Electrochemical "true" surfaces of the coatings were found to be dependent on structure and morphology: the mixtures that form a solid solution (RuO_2–TiO_2), or allow limited miscibility (IrO_2–TiO_2), show the lowest dispersion of active material. Differences in service lives, were attributed to differences in wear mechanism of the electrodes. It was found that Ti/IrO_2 (70 mol %)–Ta_2O_5 (30 mol %) is by far the best electrode.

1. Introduction

The discovery of DSA®-type electrodes has brought significant improvements in industrial electrochemistry technology, especially in the chlor-alkali industry, and has brought new hopes in the development of electrodes for oxygen evolution from acidic solutions.

In general, DSA® electrodes are characterized by a thin active coating (usually few microns) deposited on a base metal, usually a valve metal: Ti, Zr, Ta, Nb. The choice and the influence of the base metal have already been investigated and discussed in a previous paper [1]. The coating enables the electrical charge transport between the base metal and the electrode/electrolyte interface, and is chosen for its high chemical and electrochemical stability, and its ability to catalyse the desired electrochemical reaction.

DSA® anodes first showed that noble metal oxides can exhibit much better performances than those of the corresponding noble metals [2, 3], leading to the growth of a new field for applied and fundamental electrochemistry. Electrochemically active oxides such as RuO_2 and IrO_2, represent, in general, the most expensive element of a coating. When used in severe conditions, losses of active material caused by chemical or electrochemical corrosion, can make the process too expensive for technological application. Therefore, and since the beginning of DSA® electrodes, the pure oxides have been mixed with stabilizing oxides which can be either conducting (e.g. addition of IrO_2 to RuO_2 [4–6]), or non conducting (e.g. addition of TiO_2 to RuO_2 [7]). Very often this results in lower electrocatalytic activity, but in general the high operating lifetimes of such coatings make it economically variable. The non conducting oxides are especially attractive due to their considerably lower price.

In this work, nine binary mixtures composed of a conducting component (RuO_2, IrO_2 and Pt) mixed with a non conducting oxide (TiO_2, ZrO_2 and Ta_2O_5) were deposited on a Ti base (Table 1). For each combination the whole composition range of 10–100% conducting oxide was investigated for stability with accelerated life tests and the electrocatalytic activity was estimated through cyclic voltammetry. As electrocatalytic properties and behaviour under operating conditions are strongly influenced by the microstructure, the selected coatings were examined by means of XRD. The study, however, was mainly focused on the chemical and electrochemical stability of these coatings, since the goal of this work was to develop a stable, long operating DSA®-type anode for oxygen evolution in H_2SO_4 media. Today quite a few papers have been published on DSA® electrodes for oxygen evolution, including several ones on the coatings investigated here. However each paper deals with just one or two oxide combinations; moreover each laboratory has its own electrode preparation method and testing conditions, which make the comparison difficult. Several aspects such as base metal pretreatment, noble metal oxide precursors, choice of the solvent for the painting solution, preparation temperature etc., have been briefly discussed [8] showing that the microstructure, morphology, adherence and service life of the coating can be significantly altered.

Reported below is a systematic investigation for the preparation of an oxygen evolving electrode stable in acidic solutions, by using standard preparation techniques and testing conditions.

---

* To whom correspondence should be addressed.

0021-891X/91 $03.00 + .12

Table 1. Preparation conditions of the nine selected coatings

Coatings	*Metal salts*	*Solvent* and total concentration* (M)	*Annealing temperature* (°*C*)
RuO_2-TiO_2	$RuCl_3$ aq., $TiCl_3$	A 0.5	460
RuO_2-ZrO_2	$RuCl_3$ aq., $ZrOCl_2$ aq.	A 0.5	460
RuO_2-Ta_2O_5	$RuCl_3$ aq., $TaCl_5$	B 0.17	500
IrO_2-TiO_2	H_2IrCl_6 aq., $TiCl_3$	A 0.5	550
IrO_2-ZrO_2	H_2IrCl_6 aq., $ZrOCl_2$ aq.	A 0.5	550
IrO_2-Ta_2O_5	H_2IrCl_6 aq., $TaCl_5$	B 0.17	550
Pt-TiO_2	H_2PtCl_6 aq., $TiCl_3$	A 0.5	500
Pt-ZrO_2	H_2PtCl_6 aq., $ZrOCl_2$ aq.	A 0.5	500
Pt-Ta_2O_5	H_2PtCl_6 aq., $TaCl_5$	B 0.17	500

* A = H_2O – isopropanol (9 : 1) B = ethanol – isopropanol (1 : 1).

2. Choice of base metal and coating components

2.1. *Choice of a base metal*

It has been shown in a previous paper [1], that tantalum best meets the requisites for a stable, conducting anode base. Its price is nevertheless high as compared to other more conventional metals substrate like titanium, and its high oxygen affinity implies a more sophisticated preparation procedure (oxygen free atmosphere during thermal treatment). The same work also showed that zirconium cannot be expected to be a good base for DSA® coatings. On a cost/performance basis, titanium represents the best alternative and is actually used in almost all the conventional DSA® applications and was chosen as base metal for the present work.

2.2. *Choice of a conducting component of the coating*

The electrocatalytic activity for oxygen evolution at various oxide electrodes, as a function of thermodynamic or kinetic data, changes according to volcano-shaped curves [9]: showing that RuO_2, IrO_2 and Pt are among the best catalysts available for oxygen evolution in acidic media. These oxides were chosen for further investigation. Unlike the case of $RuCl_3 . xH_2O$ and $H_2IrCl_6 . xH_2O$ which thermolyse in air to the corresponding dioxide [10], thermogravimetric measurements on $H_2PtCl_6 . xH_2O$ showed that thermolysis yields $PtO_{0.12 \pm 0.05}$, i.e. almost only metallic Pt [8]. This result is in excellent agreement with previous studies [10 and references herein]. Thereafter the Pt-based compound will be noted Pt.

2.3. *Choice of a non conducting component of the coating*

It has been shown that the conducting oxides can be stabilized, and makes it more suitable for practical applications. This can be best achieved by adding to the precious metal oxide a non conducting oxide in order to increase the coatings' stability. No correlation between the type of non conductive oxides and their ability to guarantee a long operating time is reported in the literature: as a matter of fact, the effect of such oxides in binary coatings deposited on base metals has not yet been extensively studied. TiO_2, Ta_2O_5 and ZrO_2 have already been used in some cases, showing promising behaviour (see [7] for a general review, [11] for RuO_2/ZrO_2, [12] for $RuTaO_x$ and $RuIrTaO_x$, [13] for RuO_2/Ta_2O_5, [14] for IrO_2/TiO_2, [15] for IrO_2/Ta_2O_5). These oxides are semiconductors, and can easily be doped by Cl^- ions or oxygen deficiency.

3. Experimental details

3.1. *Coating preparation*

The classical coating preparation and application consist of the following steps: dissolution in a suitable solvent of the coating compounds used in the form of soluble salts; then application of the coating solution application on the pretreated base metal; solvent evaporation at low temperature (slightly above the solvent evaporation temperature) and finally thermal decomposition of the metal-containing salts into the corresponding oxide phases at high temperature in air. This procedure is repeated until the desired coating thickness is reached.

The quality of a DSA® coating prepared by this thermal decomposition technique depends on: the nature of the soluble salts and of their solvent; the concentration of the solution thus formed; the painting technique such as brush, spray or dipping; on the number and thickness of the applied coating layers and the temperature and time of annealing. As discussed in a previous paper [8], the deposition yield of some metal salts is not always 100%, and the actual coating composition on the annealed electrode, can be different from the composition of the painting solution. This is the case for Pt, whose deposition yield is about 60% (40% being lost by evaporation). All the other coatings studied in this paper have given 100% deposition yield. The compositions listed thereafter will be the effective compositions of the coatings.

3.1.1. Choice of the annealing temperature. Several metal chloride salts commercially available are given in Table 1, with their solubility in water and alcohols, with the temperature range necessary to the formation of the as indicated oxide. These temperatures were determined by thermogravimetric measurements [16, 17]. However, it has been shown [8, 18] that the thermal behaviour of a pure metal chloride is modified, if it is previously dissolved in an organic solvent, and then dried; this is also the case when two metal chloride salts are heated together to form a binary coating and should be considered when selecting the decomposition temperatures. The thermal oxidation study of titanium [1], has shown that this metal should not be treated above 560° (oxidation threshold) in order to avoid its coverage with an electrically insulating oxide film. The annealing temperatures chosen for each coating are reported in Table 1.

3.1.2. Choice of solvent. In order to obtain a uniform painting solution, all the salts should be totally dissolved. In general, water is used with 10% isopropanol in order to increase the wettability of the varnish; for the solutions containing $TaCl_5$, which decomposes in water, an organic water-free mixture is chosen: ethanol–isopropanol (1 : 1). The concentration of the solutions are calculated in order to obtain a 2–3 μm thick coating, by applying 12 layers of varnish.

3.1.3. Application technique. At a laboratory scale, the electrode surfaces used range from 1 to 5 cm^2. The easiest application technique for such samples is painting by brush which minimizes the losses of active material. Table 1 gives all the conditions chosen for the coating preparation.

3.2. *Microstructural investigation: X-ray diffraction (XRD)*

A Philips RD60/2 diffractometer, with a PW 1049/10 goniometer and a Cu PW 2103/00 tube diffraction was used. Source: Cu Kα; voltage 40 kV at 32 mA current. Angular speed of the goniometer: 1° min^{-1}.

3.3. *Accelerated life tests*

Due to their excellent chemical and electrochemical resistance under anodic polarization for chlorine or oxygen evolution, DSA®-type electrodes can reach very long operating times (up to 35 000 Ah cm^{-2} for the Ti/RuO_2–TiO_2 electrode in brine electrolysis). In order to study the performances of new electrodes on the laboratory scale, a technique of testing must be found that will artificially shorten the operating time of the anodes. This had led to the so-called "accelerated life tests", which have been widely used, and whose scope should be to provide predictive values for the operating time of electrodes used in real conditions.

The operating time of an electrode evidently depends on its wear mechanism. In order to establish a valid correlation between accelerated tests and true operating conditions, one has to be sure not to change the electrode's wear mechanism, but just to provoke an acceleration of the deactivation. It has been known for a long time that DSA® electrodes exhibit different performances depending on the operating conditions: for example the Ti/RuO_2–TiO_2 electrode shows very long operating time in concentrated chloride solutions where the main reaction is chlorine evolution, while it shows very poor performance for oxygen evolution. As the wear mechanisms are different in these cases, one should not use a test, say in H_2SO_4, if the electrode is dedicated to chlorine evolution.

In general, for service lives of DSA®-type electrodes, the following factors should be considered: the ability of the base metal to form a protective (but conducting or susceptible of being doped) layer; the effect of chemical attack by corrosive species (F^-; Br^-; CN^-; nitrites, etc.); the porosity (or roughness factor) of the coating which have an influence on the effective current density; the kinetics of the desired reaction which determines the operating potential and therefore the stability of the coating species. Thus, for a given electrode and for a given desired reaction, one has to pay attention to the combined effects of the applied current density i (which determine the working potential), the temperature and the nature of the electrolyte, on the wear mechanism.

The accelerated life tests were conducted as follows: 1 cm^2 of the electrode was polarized anodically in 30% H_2SO_4 at 80° C under galvanostatic conditions (750 mA cm^{-2}), using two zirconium cathodes as counter electrodes and the anode potential was recorded as a function of time: (reference electrode $Hg/Hg_2SO_4 . K_2SO_4$ sat.). The end of the service life for a given electrode was determined by the time at which the anode potential increased significantly (about 5 V): at this stage the electrode was said to be inactive. In order to improve the reproducibility of the results, at least five identical electrodes were used for each experiment.

3.4. *Electrochemical activity*

All cyclic voltammograms were recorded after 15 minutes of cycling at 50 mV s^{-1} with classical instrumentation, using 1 cm^2 anodes in H_2SO_4 1 M at 20° C. The anodic charges were obtained by integration of the voltammetric surfaces, between − 800 and + 800 mV against $Hg/Hg_2SO_4 . K_2SO_4$ sat., unless otherwise specified.

4. Results

4.1. *Microstructure of the coatings*

Although in the classical and well-known Ti/RuO_2–TiO_2 electrode there is only a low percentage of conducting oxide (i.e. 30 mol % RuO_2), this anode has a good electrical conductivity and a good catalytic activity for both chlorine and oxygen evolution. Its performance is attributed to the existence of a metastable solid solution between TiO_2 and RuO_2 due to their isomorphism with the rutile crystal structure.

This point is still in discussion: based on electrical conductivity measurements, an author suggests a fine mixing of conducting and insulating particles [19], rather than a true solid solution. This solid solution seems to be formed only if the coating is prepared by the thermal decomposition method of successive layers, and it is favoured by a titanium base [20, 21].

The crystalline structures of the nine anode coatings investigated were determined by XRD, and can be classified in the following groups (detailed spectra and results are given elsewhere [22]):

Solid solution (RuO_2–TiO_2). Our spectra are in excellent agreement with literature available data. The peaks of the pure oxides are not visible on the spectra but are replaced by common peaks, indicating that the distances between the crystalline planes are modified. The mixed crystals thus formed have a rutile structure. Anatase TiO_2 was found after annealing for a long time.

Solid solution with limited miscibility (IrO_2–TiO_2). The spectra show the coexistence of pure IrO_2 peaks with unidentified peaks. No pure rutile TiO_2 was found, which suggests the formation of a solid solution with partial solubility. The limited solubility of TiO_2 in IrO_2 is also reported by McDaniel [23].

Mixing of oxide crystals (RuO_2–ZrO_2, IrO_2–ZrO_2). There is no solid solution: both oxides are crystalline and the peaks correspond to the ASTM values of the pure oxides.

Mixing of oxide crystals and an amorphous phase (IrO_2–Ta_2O_5; RuO_2–Ta_2O_5). In this case one finds the peaks correspond to the pure conducting oxide and a second phase which is amorphous and therefore no characteristic peaks appear, but only broadened peaks are recorded. This is typical of Ta_2O_5, for which the annealing temperature (550° C) and the preparation conditions did not promote the crystallization [24].

Mixing of a metal and an oxide (Pt–ZrO_2, Pt–TiO_2). With the preparation conditions used, metallic Pt is formed instead of its oxide. In fact, careful thermogravimetric measurements established that on average $PtO_{0.12}$ is formed, suggesting low percentage conversion of Pt to be converted to PtO or PtO_2 [1]. High and narrow platinum peaks can be found, corresponding to a phase with a high degree of crystallinity. On the other hand, the broad peaks observed for ZrO_2 and TiO_2 suggest the existence of very fine crystalline powders.

Mixing of a metal together with an amorphous phase (Pt–Ta_2O_5). Narrow and well defined peaks of crystalline Pt coexist with the broad peaks of amorphous Ta_2O_5.

4.2. *Electrochemical activity*

The electrochemical activity of a conducting coating is related to the number of active sites accessible to the electrolyte. A means of direct investigation is cyclic voltammetry. As pointed out by other authors [12, 25], voltammetric profiles (curves) of thermally prepared oxides are not yet well understood, since a large background current is present over the entire potential range, with no well-defined double layer charging region (Fig. 1). The situation is different for platinum, whose charge, Q_H, associated with the absorption of a monolayer of hydrogen on the surface is known [26, 27]. The "true" surface area, can thus be determined by direct integration of the well-defined hydrogen adsorption region, as obtained from experimental voltammograms (Fig. 2). This method can

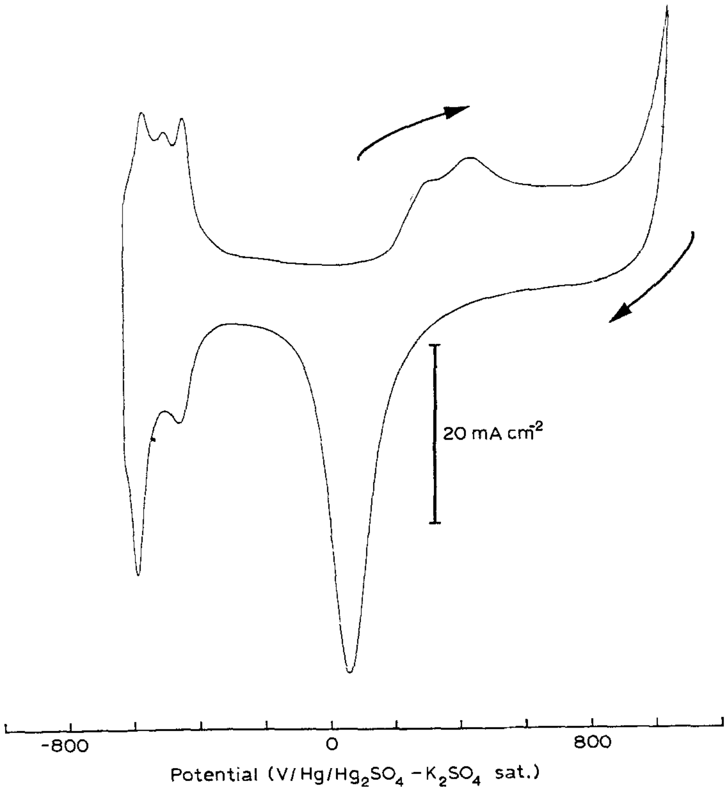

Fig. 1. Typical voltammogram of a Pt (42 mol %)–TiO_2 (58 mol %) coating. Recorded at 200 mV s^{-1}, in 1 M H_2SO_4 at 20° C, between −600 and +950 mV against Hg/Hg_2SO_4–K_2SO_4 sat.

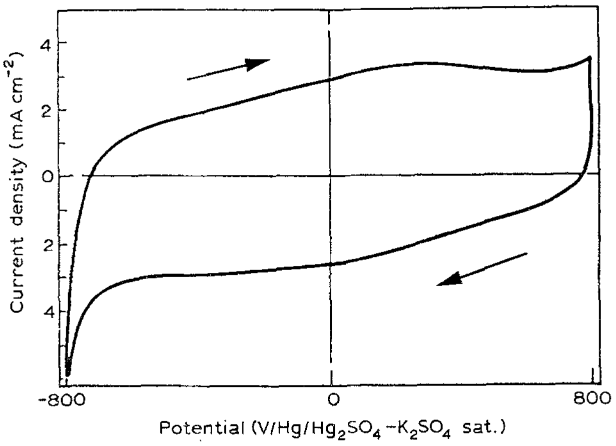

Fig. 2. Typical voltammogram of a Ti/IrO_2 (70 mol %)-Ta_2O_5 (30 mol %) electrode, recorded at 50 mV s^{-1}, in 1 M H_2SO_4 at 20° C, between −800 and +800 mV against Hg/Hg_2SO_4-K_2SO_4 sat.

also be applied to platinum-mixed oxide coatings. This was expected since the platinum-based coatings, as mentioned above, are characterized by a dispersion of large crystallites of platinum (sharp XRD peaks), so that all the corresponding voltammograms exhibit the typical hydrogen adsorption region of platinum.

In order to correlate the true surface area obtained through Q_H with the total anodic charge Q_{tot}, experiments were conducted on several platinum-based coatings with comparable platinum loadings, prepared so as to offer different qualities of platinum dispersions (Fig. 3): for electrodes 1 to 3, the inert oxide was changed from TiO_2 to ZrO_2 and Ta_2O_5; for electrode 4, the coating preparation solution was made of $H_2PtCl_6 . xH_2O$ added to a colloidal solution of TiO_2; for electrode 5 the ratio of platinum to inert oxide was lowered by a factor of 5. All voltammograms were recorded in H_2SO_4 1 M, 80° C at a potential sweep rate of 200 mV s^{-1}. The data are plotted in Fig. 3, showing a linear relationship ($r = 0.9998$) between the total anodic charge $^*Q_{tot}$, and $^*Q_H$ (both expressed per mole of platinum). Thus, in the case of platinum-based coatings, the evaluation of the electrochemical surface area through cyclic voltammetry, is straightforward.

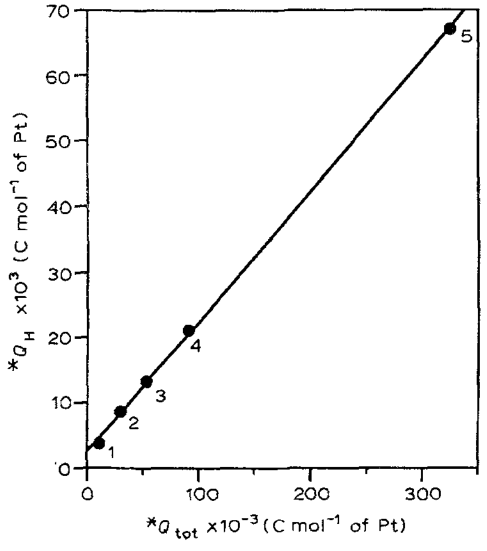

Fig. 3. Relationship between total anodic charge ($^*Q_{tot}$), and the charge associated with hydrogen adsorption ($^*Q_H$) for some Pt-based coatings: 1: Pt-Ta_2O_5; 2: Pt-ZrO_2; 3: Pt-TiO_2; 4: Pt-$TiO_{2colloidal}$; 5: *Pt-TiO_2 (*Pt-TiO_2 is a coating with much lower content of Pt).

In the case of mixed oxide coatings the question is whether to determine if the total anodic charge gives a valid evaluation of the true surface area. The answer is not trivial as several studies on RuO_2, IrO_2 [28] and RuO_2-TiO_2 [29] coatings, have shown that the total anodic charge of the voltammogram between the hydrogen and oxygen gas evolution regions, is proportional to the "true" surface area as measured either by BET or zinc adsorption [28, 30]; while other studies were inconclusive results [12]. These techniques, however, establish a correlation between the anodic charge and adsorption active sites, whereas electrochemically active sites would be more appropriate. To establish such a correlation, one must first know the electrochemical reactions, i.e. the anodic and cathodic currents that charge and discharge the active layer, and thus the electric charge transferred per active site. The major difficulty arises from the identification of the residual current recorded during cyclic voltammetry. This current obviously depends on the electrochemically active species in the coating and on the redox transitions thus involved. In the case of the more widely investigated RuO_2 based coatings, several redox transitions are known (e.g. Ru III/Ru IV, and Ru IV/Ru VI) and both purely capacitive and pseudocapacitive currents were found to coexist [12, 31–34]. Q_{tot} depends on the porosity of the coating and on a possible enrichment of the coating surface by conductive (active) species which would also result in an apparent higher surface area of the mixed oxide coatings. Figure 4 shows that for a Ti/IrO_2-TaO_5 electrode, the dependence of Q_{tot} on the catalyst loading is linear, being in agreement with the findings on RuO_2 electrodes [25, 35], but contradicting the results obtained on IrO_2 electrodes [36]. This difference might be due to differences in the electrodes preparation technique, which can lead to quite different mor-

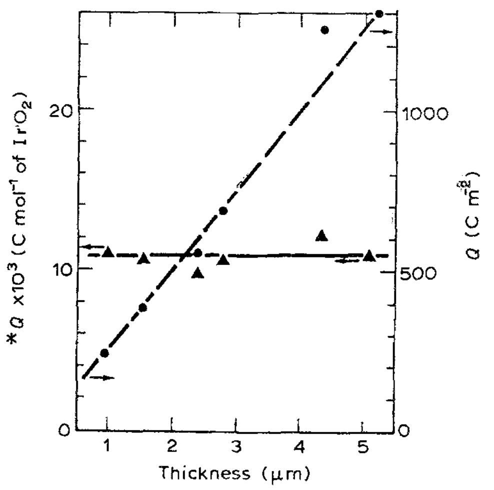

Fig. 4. Anodic charges, Q, expressed per unit of geometric area, and normalized anodic charges $^*Q$ (per mole of conducting oxide) as a function of coating thickness, for a Ti/IrO_2 (70 mol %)-Ta_2O_5 (30 mol %) electrode.

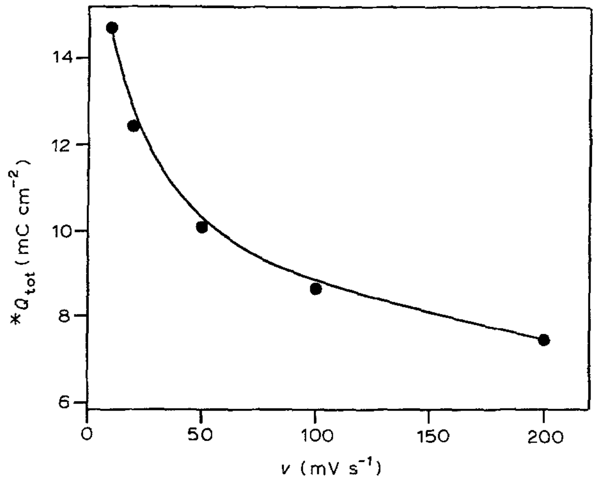

Fig. 5. Dependence of the total anodic charge Q_{tot} on potential sweep rate, for a Ti/IrO_2 (70 mol %)-Ta_2O_5 (30 mol %) electrode, in 1 M H_2SO_4. The curve was integrated between +600 mV and −600 mV.

phologies [8]. With the method as described in this paper, the coating porosity grows uniformly when loading increases. Ardizzone and Trasatti [25] confirmed recently the dependence of Q_{tot} on the potential sweep rate for RuO_2 electrodes, showing that bulk and surface contributions to the voltammetric charge coexist. This was explained, for high sweep rates, by a limitation of the diffusion of proton donating species to the reactive sites in the bulk of the coating. This was also observed with the Ti/IrO_2–TaO_5 electrode as shown in Fig. 5. It should be noted that the electrode was "activated" for 1 h at 1 A cm^{-2} prior to measurements, since it is known that during the initial cycling, the voltammetric charge increases until it reaches a maximum, constant value, after several minutes of cycling.

Figure 6 shows the evolution of anodic currents measured at several potentials, as a function of potential sweep rate, for IrO_2–Ta_2O_5 voltammograms. The linearity is typical of a capacitance, and at −0.6 V the slope is 9.7 mF cm^{-2} which is in good agreement with capacitances of surface films [37]. At more positive potentials, the values found are too high (Table 2), although strict linearity between current density and sweep rate is observed. Integration of the charge incorporated by the electrode at 200 mV s^{-1} against the potential (Fig. 7), confirms that the charging process is not purely capacitative: the linear relationship obtained indicates that the charging process is in fact associated with a slow step, limited by mass transport. This behaviour suggests that both purely capacitive and pseudocapacitive currents are involved [12]. It should be noted, however, that Fig. 7 was obtained at a sweep rate of 200 mV s^{-1} which involves, on the basis of Fig. 5, only the "outer" surface where the proton exchange process is easier.

Table 2. Capacitances of a IrO_2–Ta_2O_5 coating, calculated from the current density–sweep rate relationships given in Fig. 6

Potential (*V*)	*Capacitance* (*mF cm*$^{-2}$)
−0.6	9.7
−0.2	20.9
+0.2	38.5
+0.6	44.7

At the present stage, it seems that, based on the above discussed results, crude Q_{tot} values should not be used for the determination of the real electrochemical surface of mixed oxide coatings. Neverthless, the excellent reproducibility of our experiments suggests that relative values of Q_{tot} can be compared, if the same conducting oxide in the coating is involved. On this basis, and keeping in mind that the electrochemical characteristics of IrO_2 and RuO_2 are different from those of platinum, we will admit that the total anodic charge, $*Q_{tot}$, of all the tested coatings, is a valid indication of the degree of dispersion of the catalyst in the coating. The absolute values of anodic charge for RuO_2, IrO_2 and platinum should not be directly compared.

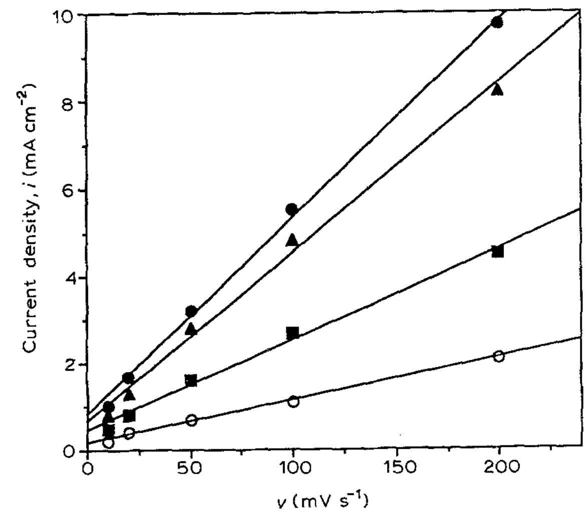

Fig. 6. Capacitative charging currents against sweep rate, measured on cyclic voltammograms of a Ti/IrO_2 (70 mol %)-Ta_2O_5 (30 mol %) electrode, at several potentials: (○) −0.6, (■) −0.2, (▲) +0.2 and (●) +0.6 V. The capacitances given by the slopes are reported in Table 2. Conditions as for Fig. 2.

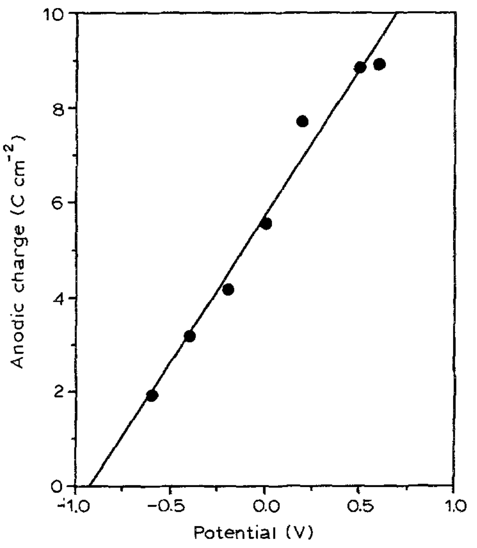

Fig. 7. Anodic charge incorporated at 200 mV s^{-1} by the Ti/IrO_2 (70 mol %)-Ta_2O_5 (30 mol %) electrode, as a function of the potential. Conditions as for Fig. 2.

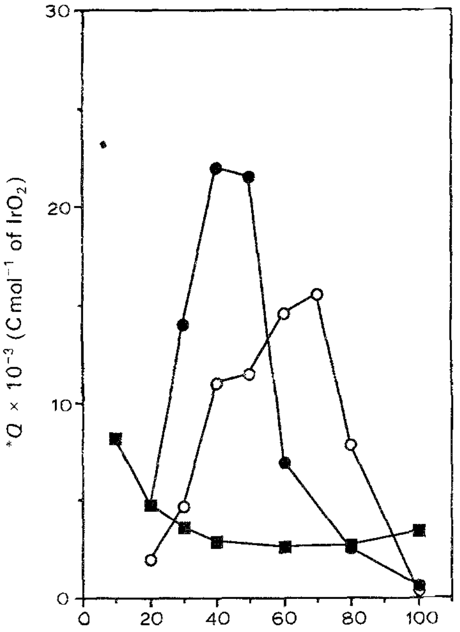

Fig. 8. Electrocatalytic activity $*Q$ of IrO_2-based coatings as a function of IrO_2 content. Experimental conditions as for Fig. 2. (○): IrO_2-Ta_2O_5; (■): IrO_2-TiO_2; (●): IrO_2-ZrO_2.

Figures 8 to 10 give the anodic charges per mole of conducting oxide, $*Q_{tot}$, measured by cyclic voltammetry as a function of the respective conducting oxide content. Tables 3 and 4 give the compositions showing the highest electrocatalytic activity and the corresponding values of anodic charge. All the coatings show a maximum of anodic charge.

4.3. *Anodic stability*

It is known that the addition of a non conducting oxide, into the active coating can improve the anodic stability of DSA® electrodes: coatings with various concentrations of the non conducting oxide were prepared and tested in order to determine their optimal composition.

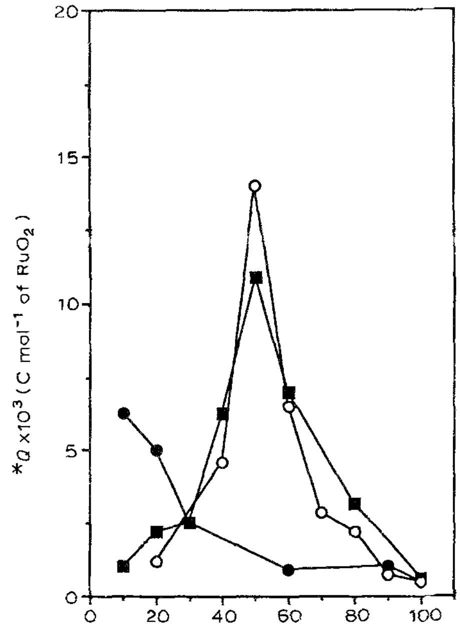

Fig. 9. Electrocatalytic activity $*Q$ of RuO_2-based coatings as a function of RuO_2 content. Experimental conditions as for Fig. 2. (○): RuO_2-ZrO_2; (■): RuO_2-Ta_2O_5; (●): RuO_2-TiO_2.

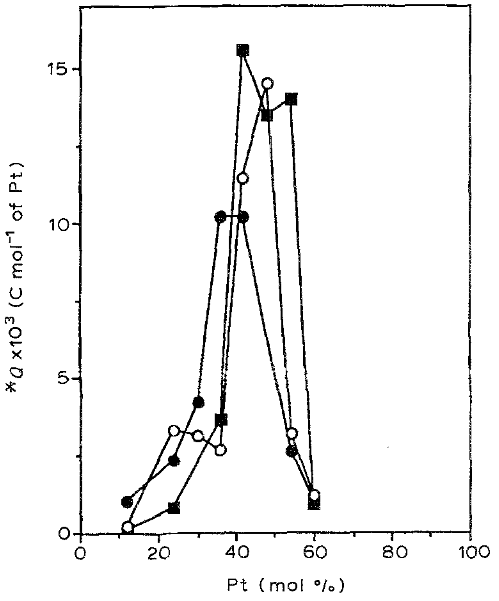

Fig. 10. Electrocatalytic activity $*Q$ of Pt-based coatings as a function of Pt content. Experimental conditions as for Fig. 2. (○): Pt-ZrO_2; (■): Pt-Ta_2O_5; (●): Pt-TiO_2.

Figure 11 shows that, for a Ti/IrO_2-Ta_2O_5 electrode, the relation between the total amount of coating and the service life is not linear. A similar result is reported for the Ti/RuO_2-TiO_2 electrode [38]. By calculating the efficiencies, in A h mol^{-1} of conducting oxide, it appears that under the present experimental conditions, a maximum occurs for a 1.5 μm thick coating. Once again, and because of the porous nature of the coating, all the active sites are not equivalent, (i.e. do not transfer the same amount of electrical charge) as in the case of the coexistence of an inner and an outer layer. The similarity with the conclusions drawn from CV experiments is only apparent since in the latter, the charges were transferred without gas evolution, while in these lifetime tests, oxygen is evolved and the bubbles formed inside the coating volume prevent new electrolyte from reaching the inner active sites.

Figures 12 to 14 give the results of the accelerated life tests as a function of the composition for all the samples. The lifetime is given in terms of efficiency, in order to compare the real performances of the various coatings. These values correspond to the real anode efficiency since the total electrical charge crossing the

Table 3. Electrocatalytic activity: coating compositions showing maximum anodic charge, as measured by cyclic voltammetry

Inert oxide	*Conducting oxide (mol %)*		
	RuO_2	*IrO_2*	*Pt*
TiO_2	10	10	36–42
ZrO_2	50	40	48
Ta_2O_5	50	70	42

*Table 4. Electrocatalytic activity: maximums of anodic charge *Q (per mole of conducting oxide)*

Coating	*Anodic Charge *Q × 10^3 ($C mol^{-1}$)*		
	RuO_2	*IrO_2*	*Pt*
TiO_2	6.3	8.2	17
ZrO_2	14	22	24.2
Ta_2O_5	10.9	15.5	26

electrode is divided by the total amount of the active component. The curve for IrO_2–Ta_2O_5 on Fig. 12 is a typical example where the dilution of the conducting oxide by an inert oxide increases significantly the anodic stability. The RuO_2–ZrO_2 system (Fig. 13) is the only case where the addition of a non conducting metal oxide lowers the stability of the coating. In other cases (e.g. RuO_2–Ta_2O_5) the optimum lies within a large domain of composition.

Table 5 gives the compositions of maximum anodic stability for each coating, and Table 6 gives the corresponding efficiencies.

5. Discussion

It can be seen from Tables 3 to 6 that the optimum compositions, except for platinum based coatings are neither determined by the nature of conducting nor the inert oxide taken separately, but are influenced by both. The respective optimal compositions for the anodic stability and the catalytic activity are different, the dilution by an inert oxide being beneficial in all cases. The efficiencies shown in Table 6 reflect the electrochemical stability sequence of the conducting component: $IrO_2 > Pt > RuO_2$. Similarly, within a family based on the same conducting compound, we expected the stability sequence to follow the chemical stability of the inert (non conducting) oxides, i.e. $Ta_2O_5 > TiO_2 > ZrO_2$. Table 6 shows that this is only confirmed for IrO_2-based coatings. This can be explained by considering the differences in the wear mechanism of the electrodes. In the aggressive conditions of the tests, important losses of RuO_2 occur through oxidation to soluble RuO_4^{2-} or to volatile RuO_4 [29]. Pt is also known to undergo dissolution [39], but to a lesser extent, while IrO_2 is sufficiently stable so that the deactivation occurs through dissolution of the base or building up of a non conducting layer between the coating and the base. Each time an active site of RuO_2 or Pt is dissolved, the coating composition changes with an enrichment in inert oxide. This causes the potential to increase, leading to an acceleration of the active material dissolution. For IrO_2 electrodes, the sequence is determined by the ability of the inert oxide to protect the base metal, while for RuO_2 and Pt coatings the sequence is determined by the ability of the inert oxides to stabilize the conducting oxide, as in the case of RuO_2–TiO_2 where

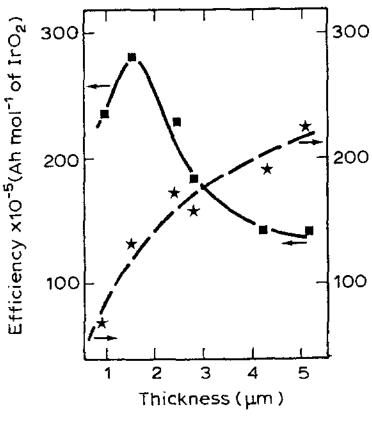

Fig. 11. Service life and efficiency of a Ti/IrO_2 (70 mol %)–Ta_2O_5 (30 mol %) electrode, as a function of the coating thickness. Conditions: 30% H_2SO_4, 80°C, 750 mA cm^2.

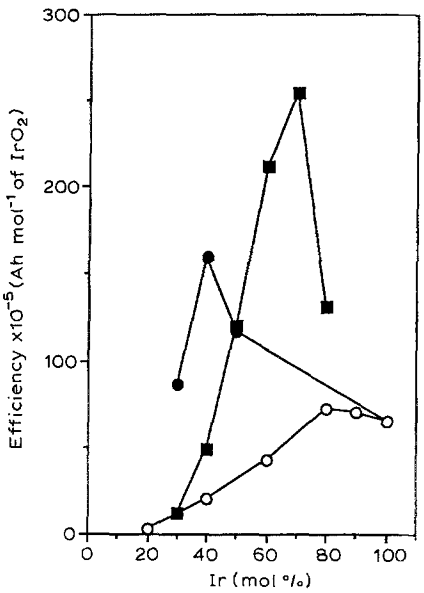

Fig. 12. Anodic stability of IrO_2-based coatings as a function of IrO_2 content. Experimental conditions as for Fig. 10. (○): IrO_2–ZrO_2; (■): IrO_2–Ta_2O_5; (●): IrO_2–TiO_2.

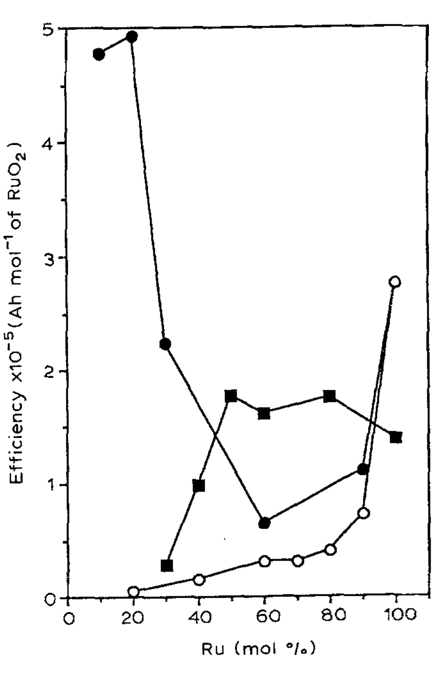

Fig. 13. Anodic stability of RuO_2-based coatings as a function of RuO_2 content. Experimental conditions as in Fig. 10. (○): RuO_2–ZrO_2; (■): RuO_2–Ta_2O_5; (●): RuO_2–TiO_2.

Table 5. Anodic stability: coating compositions showing maximum efficiency, as measured by accelerated life tests

Inert oxide	*Conducting oxide (mol %)*		
	RuO_2	*IrO_2*	*Pt*
TiO_2	20	40	42
ZrO_2	100	80	36
Ta_2O_5	50-100	70	42

the maximum protecting efficiency occurs around 20 mol % RuO_2, well within the composition range of the solid solution. An exception occurs if the inert oxide itself is unstable under anodic polarization (e.g. ZrO_2), causing a rapid deterioration of the bulk oxide lattice.

Since an excellent stability can be obtained by adding Ta_2O_5 to the conducting oxide, the improved stability cannot be simply justified by the isomorphs between the base metal oxide and the non conductive oxide as would be the case with TiO_2 on titanium.

It also appears that, unlike the efficiencies, the anodic charges are within the same order of magnitude, indicating that the degree of dispersion of the catalysts in the active layer is not the only parameter responsible for the anode lifetimes. The anodic charge of the RuO_2-TiO_2 and IrO_2-TiO_2 systems (Figs 8 and 9), behave differently from the others. The reason for the existence of maximums in anodic charge, is not well understood; for binary conducting–insulating systems, the maxima might be explained by the percolation theory [40, 41]. In order to be electrochemically active, a cluster of conducting oxide must be connected to the metal base (electrons collector), and at the same time, in contact with the electrolyte. For low concentrations of such clusters, many of them are either isolated from the conducting network (also called the backbone, Fig. 15a) or do not contact the solution, being surrounded by inert oxide (such a figure is called a dead end, Fig. 15b): in both cases the clusters do not participate in the electrochemical activity of the coating. With increasing concentration of conducting oxide, the electrochemical surface increases as more particles become part of the backbone at the electrolyte interface. The anodic charges, defined by the ratio between the number of clusters in contact with the electrolyte (charge measured by C.V.) and the total amount of conducting oxide in the coating, reaches a maximum for a critical concentration, above which additional clusters occupy inner places (Fig. 15c), not contributing to the active surface increase.

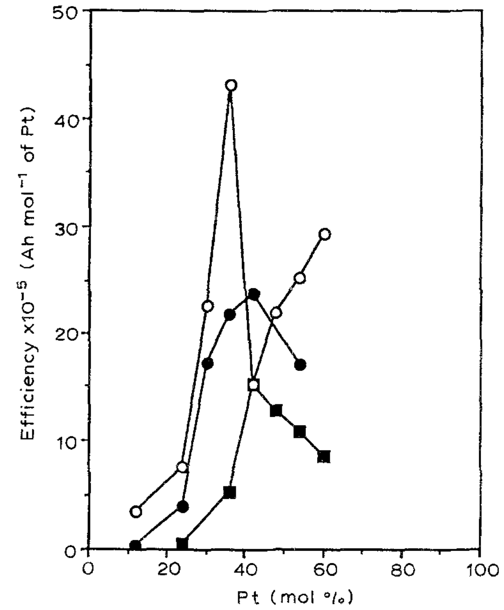

Fig. 14. Anodic stability of Pt-based coatings as a function of Pt content. Experimental conditions as for Fig. 10. (○): Pt-ZrO_2; (■): Pt-Ta_2O_5; (●): Pt-TiO_2.

Table 6. Anodic stability: maxima of efficiencies (per mole of conducting oxide)

Coating	*Efficiency × 10^{-5} ($Ah\,mol^{-1}$)*		
	RuO_2	*IrO_2*	*Pt*
TiO_2	4.9	160	23.8
ZrO_2	2.8	72	43.1
Ta_2O_5	1.8	254	15.3

The optimum compositions for RuO_2-TiO_2 and IrO_2-TiO_2 coatings, are characterized by an exceptional low content of conducting oxide, which can be explained by the formation, of a solid solution and a solid solution with limited miscibility. In these cases the coating becomes conductive and therefore the maximum of surface is obtained by using smaller amounts of conducting oxide. By adding more conducting oxide, the charge per atom decreases and moreover, one leaves the composition range of the solid solution. As a whole it seems that systems which

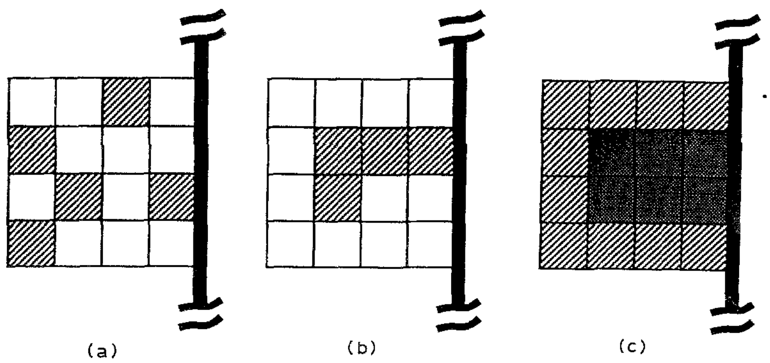

Fig. 15. Electrochemical surface of binary coating: effect of inert oxide concentration. A cluster of coating is deposited on a Ti base (in black), and is surrounded by electrolyte. Dark squares: conducting oxide; white squares: inert oxide. (a) the conducting particles are not connected to the base (electron collector); (b) they do not reach the solution; (c) only the outer particles contribute to the electrocatalytic activity.

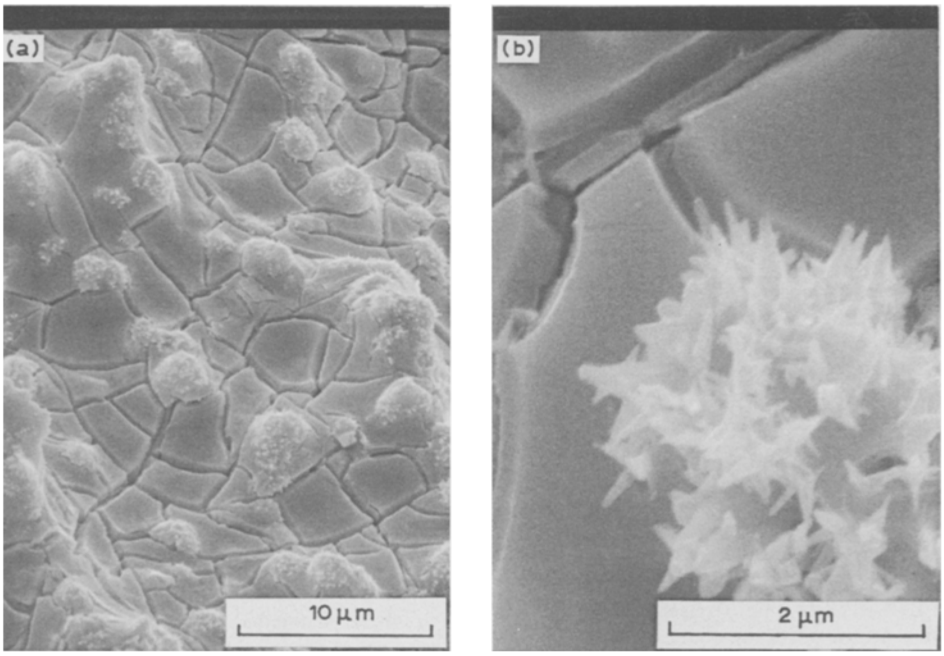

Fig. 16. SEM micrographs of a Ti/IrO_2 (70 mol %)-Ta_2O_5 (30 mol %) electrode. (a) × 5000; (b) × 14000.

form a solid solution, should be avoided if high electrochemical activities are wanted.

It is also interesting to note that most of the coatings show a maximum of the anodic charge around 50 ± 10 mol % of conducting oxide, indicating that a percolating network might indeed be responsible for the observed maxima. Exceptions to this are the two systems which form solid solutions, and the IrO_2-Ta_2O_5 system, which, due to the amorphous morphology of this coating cannot be crystallographically described. A typical cobblestone morphology was found for all the coatings, with both oxides being intimately mixed: the percolating network seems to be a good model to describe such systems. The situation is different for the IrO_2-Ta_2O_5 coating where part of the IrO_2 is in the form of needles [8] and the rest being dispersed in the cobblestones, i.e. the amorphous phase (Fig. 16). In this case the maximum in anodic charge is determined by the density of the needle on the coating surface. This particular morphology could also be responsible for the results shown in Fig. 5, with an outer region easily accessible to protons (IrO_2 aggregates), and an inner region containing less accessible sites (cobblestones).

6. Conclusion

The objective of this research program was to develop an improved DSA® electrode for oxygen evolution in concentrated H_2SO_4 solutions. Nine binary oxides based on Ru, Ir, Pt oxides mixed with Ti, Ta, Zr oxides have been characterized by investigating their crystal structure, electrochemical activity and anodic stability. The stability of such coatings was found to be mainly dependent on the anodic stability of the conducting oxide alone. It also depends on the stability of the non conducting oxide its ability to protect the base metal. The formation of solid solutions (RuO_2-TiO_2, IrO_2-TiO_2) seems to be a severe hindrance for high electrocatalytic surfaces. In practical application, this decrease of electrochemical activity is compensated by the stabilizing effect of the non conduction.

It has been found that the Ti/IrO_2 (70 mol %)-Ta_2O_5 (30 mol %) was by far the best electrode of the nine systems tested for the purpose of this work. The highest service life and the highest catalyst dispersion are associated with this composition.

References

[1] G. P. Vercesi, J. Rolewicz, Ch. Comninellis, E. Plattner and J. Hinden, *Thermochim. Acta*, submitted.
[2] H. B. Beer, US Appl. 549 194 (1966), US 3 632 498 (1972) and US 3 711 385 (1973).
[3] O. De Nora, A. Nidola, G. Trisoglio and G. Bianchi Brit. Pat. 1 399 576 (1973).
[4] R. Hutchings, K. Müller, R. Kötz and S. Stucki, *J. Mat. Sci.* **19** (1984) 3987.
[5] R. Kötz and S. Stucki, *Electrochim. Acta* **31** (1986) 1311.
[6] C. Angelinetta, S. Trasatti, Lj. D. Atanasoska, Z. S. Minevski and R. T. Atanasoski, *Mater. Chem. Phys.* **22** (1989) 499.
[7] S. Trasatti, 'Electrodes of Conductive Metallic Oxides', Elsevier, Amsterdam (1981).
[8] Ch. Comninellis and G. P. Vercesi, *J. Appl. Electrochem.*, submitted.
[9] S. Trasatti, *Electrochim. Acta* **29** (1984) 1503.
[10] G.-W. Jang and K. Rajeshwar, *J. Electrochem. Soc.* **134** (1987) 1830.
[11] L. D. Burke and M. McCarthy, *Electrochim. Acta* **29** (1984) 211.
[12] R. S. Yeo, J. Orehotsky, W. Visscher and S. Srinivasan, *J. Electrochem. Soc.* **128** (1981) 1900.
[13] A. De Battisti, G. Lodi, M. Cappadonia, G. Battaglia and R. Kötz, *J. Electrochem. Soc.* **136** (1989) 2596.
[14] T. V. Varlamova, I. D. Belova, R. R. Shrifina, B. Sh. Galyamov, Yu. E. Roginskaya and Yu. N. Venetsev, *Zh. Fiz. Khim.* **64** (1990) 385.
[15] J. Kolb, C. R. Franks and B. A. Schenker, US Pat. 3 793 164.
[16] J. Rolewicz, Ch. Comninellis, E. Plattner and J. Hinden, *Electrochim. Acta* **33** (1988) 573.
[17] *Idem, Chimia* **42** (1988) 75.
[18] F. Hine, M. Yasuda and Y. Yoshida, *J. Electrochem. Soc.* **124** (1977) 500.

[19] W. A. Gerrard and B. C. H. Steele, *J. Appl. Electrochem.* **8** (1978) 417.
[20] Yu. E. Roginskaya, V. I. Bystrov and D. M. Shub, *Zh. Neorg. Khim.* **22** (1977) 201.
[21] V. M. Lebedev, Yu. E. Roginskaya, N. L. Klimsenko, V. I. Bystrov and Yu. N. Venetsev, *ibid.* **21** (1976) 1380.
[22] J. Rolewicz, Doctoral thesis, Swiss Federal Institute of Technology, Dept. of Chem. Ingen., Thesis No. 662 (1987).
[23] C. L. McDaniel and S. J. Schneider, *J. Res. Nat. Bur. Stand.* **71A** (1967) 119.
[24] Ch. Comninellis, G. P. Vercesi and J. Hinden, *Electrochim. Acta*, submitted.
[25] S. Ardizzone, G. Fregonara and S. Trasatti, *Electrochim. Acta* **35** (1990) 263.
[26] A. M. Feltham and M. Spiro, *Chem. Rev.* **71** (1971) 177.
[27] T. Biegler, D. A. Rand and R. Woods, *J. Electroanal. Chem.* **29** (1971) 269.
[28] R. F. Savinell, R. L. Zeller III and J. A. Adams, *J. Electrochem. Soc.* **137** (1990) 489.
[29] D. V. Kokoulina, T. V. Ivanova, Yu. I. Krasovitskaya, Z. I. Kudryavtseva and L. I. Krishtalik, *Soviet Electrochem.* **13** (1977) 1293.
[30] L. D. Burke, O. J. Murphy, J. F. O'Neill and S. Venkatesan, *J.C.S. Faraday I* **73** (1977) 1659.
[31] S. Trasatti and G. Buzzanca, *J. Electroanal. Chem.* **29** (1971) App. 1.
[32] D. Galizzoli, F. Tantardini and S. Trasatti, *J. Appl. Electrochem.* **5** (1975) 203.
[33] T. Arikado, C. Iwakura and H. Tamura, *Electrochimica Acta* **22** (1977) 513.
[34] K. Doblhofer, M. Metikos, Z. Ogumi and H. Gerischer, *Ber. Bunsenges. Phys. Chem.* **82** (1978) 1046.
[35] L. D. Burke and O. J. Murphy, *J. Electroanal. Chem.* **96** (1979) 19.
[36] S. Ardizzone, A. Carugati and S. Trasatti, *ibid.* **126** (1981) 287.
[37] S. Trasatti, *Electrochim. Metall.* **2** (1967) 12.
[38] C. Iwakura, M. Inai, M. Manabe and H. Tamura, *Denki Kagaku* **48** (1980) 91.
[39] C. G. Smith and Y. Okinaka, *J. Electrochem. Soc.* **130** (1983) 2149.
[40] D. Stauffer, *Phys. Rep.* **54** (1979) 1.
[41] 'The Mathematics and Physics of Disordered Media', Proceedings of a Workshop, Minneapolis, (edited by B. D. Hughes and B. W. Ninham), in 'Lecture Notes in Mathematics' (edited by A. Dold and B. Eckmann) vol. 1035, Springer-Verlag, Heidelberg (1983).